PRIMARY PROCESSES IN PHOTOLYSIS OF OCTOPUS RHODOPSIN

HIROYUKI OHTANI,* TAKAYOSHI KOBAYASHI,* MOTOYUKI TSUDA,‡ AND THOMAS G. EBREY§
*Department of Physics, Faculty of Science, University of Tokyo, Hongo, Bunkyo-ku, Tokyo 113, Japan; ‡Department of Physics, Sapporo Medical College, Minami 1 Nishi 17, Chuo-ku, Sapporo 060, Japan; and §Department of Physiology and Biophysics, University of Illinois, Urbana, Illinois 61801

ABSTRACT The photolysis of octopus rhodopsin was studied by picosecond time-resolved spectroscopy at physiological temperature (8°C) and by steady-state spectroscopy at very low temperature (10 K). Both hypsorhodopsin and bathorhodopsin were formed from a bathorhodopsin-like red-shifted intermediate "primerhodopsin," which was the primary photoproduct with our time resolution (36 ps). Though it was proposed that hypsorhodopsin is formed solely by a multiphoton process, the present results obtained by using blue light pulses (461 nm) of low intensity showed that hypsorhodopsin is formed by a single photon mechanism via thermal decay from primerhodopsin. When the excitation intensity is increased, a channel for the photochemical formation of hypsorhodopsin from primerhodopsin is opened. There are two thermal pathways leading from primerhodopsin. One process is the formation of hypsorhodopsin, which is later thermally converted to bathorhodopsin, and the other is the direct formation of bathorhodopsin from primerhodopsin. The formation efficiencies at room temperature of hypsorhodopsin and bathorhodopsin at very low excitation intensity were estimated to be larger than 0.6 and smaller than 0.4, respectively. The formation of hypsorhodopsin was also found in the early stages of the irradiation of octopus rhodopsin with weak continuous light at 10 K. However bathorhodopsin is formed three times more efficiently than hypsorhodopsin at 10 K.

At physiological temperatures the formation of hypsorhodopsin in D_2O takes place more slowly than in H_2O. This indicates that the lifetime of primerhodopsin is decreased by H_2O/D_2O exchange. The rate constant for the primerhodopsin → bathorhodopsin conversion is more sensitive than that for the primerhodopsin → hypsorhodopsin conversion. The transformation of hypsorhodopsin to bathorhodopsin shows no deuterium effect at low temperature.

INTRODUCTION

The primary event in vision is a *cis-trans* photoisomerization of rhodopsin's chromophore, retinal (2, 3). The photobleaching of rhodopsin consists of a set of sequential thermal reactions initiated by absorption of photons. Several intermediates in this transformation have been found by low-temperature spectroscopy (4). Most of them were also found by flash or laser photolysis at physiological temperatures. The current problems are (*a*) the sequence among three intermediates formed in the picosecond region, bathorhodopsin (5), hypsorhodopsin (4), and a red-shifted precursor (6–8) called Batho' (9) or photorhodopsin (10), and (*b*) the mechanism by which the *cis-trans* isomerization is achieved.

Bathorhodopsin was first identified in the photolysis of bovine rhodopsin at 87 K by Yoshizawa and Kitô (5). The formation of bovine bathorhodopsin at room temperature occurs within 6–9 ps after the excitation of rhodopsin at 530 nm (11–13).

Hypsorhodopsin was found by continuous irradiation of bovine rhodopsin at liquid helium temperatures (4). Hypsorhodopsin is thermally converted to bathorhodopsin at temperatures higher than 20–40 K, depending on rhodopsin species (bovine, T_c = 23 K [4]; squid, T_c = 35 K [14]; octopus, T_c = 45 K [15]), and hence it is a candidate for a precursor of bathorhodopsin. However, bathorhodopsin is formed much more efficiently than hypsorhodopsin at liquid helium temperature by weak light irradiation (15).

Hypsorhodopsin was first observed at room temperature by picosecond photolysis of squid rhodopsin with 347-nm light (16, 17). Hypsorhodopsin was formed within 20 ps (the pulse width of the excitation light) and its lifetime (45 ± 10 ps) agrees with the formation time constant of bathorhodopsin (50 ± 10 ps) within experimental error. It was concluded that hypsorhodopsin is a precursor of bathorhodopsin at room temperature.

Kobayashi (7, 8) found a bathorhodopsin-like red-shifted precursor, which corresponds to Batho' (6, 9), by the picosecond photolysis of bovine rhodopsin at room temperature. The precursor was initially considered to be

This work was partly reported in Ohtani et al. (1).

Dr. Ohtani's present address is Hamamatsu Photonics K. K. Tsukuba Research Laboratory, Toyosato-machi, Tsukuba-gun, Ibaraki 300-26, Japan.

Correspondence should be addressed to Dr. Kobayashi.

the lowest excited singlet state in rhodopsin. He determined the time constants for the precursor → hypsorhodopsin and hypsorhodopsin → bathorhodopsin conversions to be 15 ± 5 ps and 50 ± 20 ps, respectively. He also mentioned that there is a minor pathway for the direct formation of bathorhodopsin from the red-shifted precursor.

Recently Shichida et al. (10) measured a transient spectrum of a similar red-shifted precursor, and called it "photorhodopsin." From the excitation intensity dependence of the absorbance change of rhodopsin (18), they proposed that hypsorhodopsin is a photoproduct of photorhodopsin. However they did not clarify whether or not the thermal formation of hypsorhodopsin occurs because at their excitation wavelength (532 nm) photorhodopsin is efficiently excited even at low excitation intensities.

To avoid this ambiguity, we used a picosecond light pulse at the wavelength of 461 nm at which the absorption cross-section of rhodopsin is 2.7 times larger than that of the red-shifted precursor. The absorption spectrum of the red-shifted precursor is similar to that of bathorhodopsin, shown in Fig. 1. A weak excitation light (35 ± 5 μJ) was used to avoid multiphoton events such as two-photon absorption of rhodopsin (19) and absorptions of a second photon by rhodopsin in the excited state and intermediates. Weak signals were measured with a highly sensitive picosecond time-resolved spectroscopy apparatus (20). Hypsorhodopsin was found even under the low photon density excitation (0.3 photons/molecule) by the 461-nm picosecond pulse. We also performed a photolysis experiment on octopus rhodopsin with continuous irradiation at 10 K. Though bathorhodopsin is a major product at low temperature, hypsorhodopsin was also found in the early stages of the irradiation at low temperatures.

MATERIALS AND METHODS

Preparation of Octopus Rhodopsin

Live octopuses (Mizudako, *Paroctopus defleini*) were decapitated in dim light, and their eyeballs removed and kept in the dark at −80°C. The thawed octopus eyes were hemisected and the isolated retinas suspended in modified cephalopod physiological saline, buffer A (400 mM KCl, 5 mM $MgCl_2$, 1 mM $CaCl_2$, 5 mM Tris [pH 7.4], 1 mM dithiothreitol, and 0.2 mM phenylmethyl sulfonyl fluoride). The microvillar membranes were isolated by a method similar to that described previously (21). The outer segment membranes were isolated by repeated sucrose flotation (37%, wt/vol, the same buffer as above) until a black pellet could no longer be found at the bottom of the centrifuge tube. The final supernatant was then diluted with an equal volume of buffer A and centrifuged. The pellet was washed four times with buffer A and four times with buffer B (5 mM Tris/HCl [pH 7.2], 1 mM dithiothreitol, and 0.2 mM phenylmethyl sulfonyl fluoride). The pellet from these washings gave two distinct layers. The upper layer was sonicated or solubilized by 2% digitonin and 2% L-1690 (lauryl ester of sucrose) (22). The resulting solution was concentrated by centriflow (Amicon Corp., Danvers, MA). Deuterated photoreceptor membranes were prepared by suspending the microvillar membranes in D_2O for 1 h. The sample was centrifuged; this procedure was repeated three times. Deuterated glycerol and digitonin were used as the solvents for deuterated samples. The absorbance of samples for the picosecond experiments was 1.2 at the excitation wavelength 461 nm (2-mm light path length).

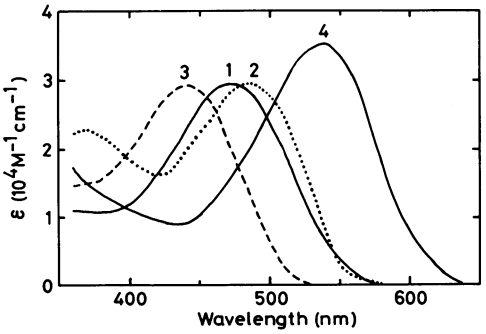

FIGURE 1 Absorption spectra of octopus rhodopsin (R), hypsorhodopsin (H), and bathorhodopsin (B). Curve *1*, R at 10°C; curve *2*, R at 10 K; curve *3*, H at 10 K; and curve *4*, B at 10 K. Spectra of B and H are reconstructed from the spectra of the photo-stationary state at 10 K (15).

Picosecond Spectroscopy Apparatus

Fig. 2 shows the block diagram of the picosecond spectroscopy apparatus used in the present study. A light source was a mode-locked Nd:YAG laser (1,064 nm, model YG 472; Quantel International Inc., Santa Clara, CA). An acoustoptic modulator (model ML-70B, 69.804 MHz; IntraAction) and a saturable absorber (Kodak 9740 in chlorobenzene) were used for hybrid mode-locking. The energy of the amplified single pulse with a two-stage amplifier was 60 mJ and the short-term stability of the peak power is within ±12%. The first anti-Stokes Raman scattering light (461 nm, 5 μJ) was generated by focusing the second harmonic of the Nd:YAG laser (532 nm) into acetone. The 461-nm pulse was amplified about 20 times by an amplifier (coumarine 440 in methanol) pumped by the third harmonic (355 nm) of the mode-locked Nd:YAG laser, and used for the excitation of samples. The width of the excitation pulse was measured to be 20 ± 1 ps (fwhm) with a streak camera (model C1370 Temporal Disperser and C1330 Temporal Analyzer; Hamamatsu Photonics K. K., Hamamatsu City, Japan). An amplified spontaneous emission was eliminated by an interference filter (460 nm, 15-nm fwhm). The intensity

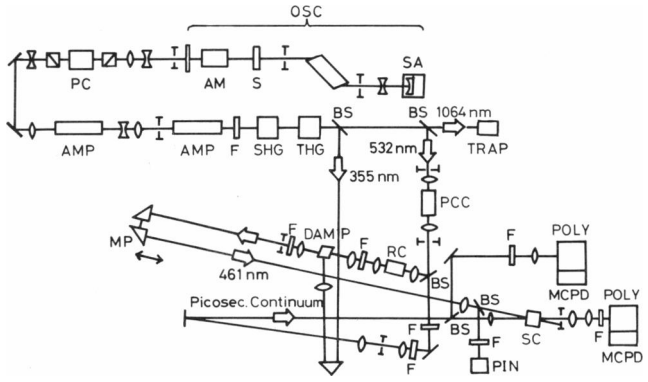

FIGURE 2 Block diagram of picosecond time-resolved absorption spectroscopy apparatus. OSC, mode-locked Nd:YAG laser; SA, saturable absorber; AM, acoustoptic modurator; PC, Pockels cell; F, filter; AMP, Nd:YAG amplifier; SHG, KDP crystal for the second harmonic generation; THG, KDP crystal for the third harmonic generation; S, shutter; BS, beam splitter; PCC, picosecond continuum generation cell; RC, Raman cell; DAMP, dye amplifier; MP, movable prism for optical delay line; PD, PIN photodiode for excitation energy monitor; SC, sample cell; POLY, polychromator; MCPD, multichannel photodiode array.

of the excitation pulse was monitored by a PIN photodiode (model S1188-01; Hamamatsu Photonics K. K.) calibrated with a power meter (model 361; Scientec, Inc., Boulder, CO). The probe was picosecond continuum light generated by focusing the second harmonic into CCl_4 or by focusing the fundamental into D_2O. The excitation and probe pulses were focused onto a sample cell (2-mm light path length). Their polarizations were parallel to each other. However, the observed kinetic behaviors are not affected by the polarization properties because the rotational motion of rhodopsin is small in picosecond time region. The diameters of the focused areas of excitation and probe pulses were 1.5 and 0.5 mm, respectively. The probe light was detected by a multichannel photodiode array (MCPD, 512 channels; Union Giken, Osaka, Japan) coupled with a polychromator (f = 20 cm, 600 grooves/mm of grating; Union Giken). 30–40 pairs of excitation and nonexcitation data were averaged by the computer system (20).

The temperature of the sample was kept constant at 8°C with a semiconductor cooling device. Acid metarhodopsin formed by the irradiation of the excitation light pulse is stable at 8°C (21). Rhodopsin was recovered from acid metarhodopsin by the irradiation with a tungsten lamp through a cut-off color filter (model 058; Hoya Corp., Akishima, Japan) after every excitation laser exposure.

Low Temperature Spectroscopy

Microvillar membranes in H_2O or D_2O were sonicated and mixed with glycerol or deuterated glycerol (1:3 vol/vol). The mixture in a 2-mm path length cell was placed in a dewar (model 10DT Super Varitemp Optical Dewar; Janis Research Co., Wilmington, MA). Absorption spectra were measured with a spectrophotometer (Cary 14; Applied Physics Co., Monrovia, CA).

RESULTS

Picosecond Spectroscopy at Physiological Temperature

Fig. 3 shows the difference absorption spectra after the 461-nm excitation of octopus rhodopsin in both the H_2O (*solid curve*) and D_2O (*dotted curve*) suspensions at 8°C. The large absorbance change around 460 nm was due to the scattering of the excitation light. The decrease in absorbance in the 415–445-nm region at 0 ps in both the H_2O and D_2O suspensions is due to the formation of a transient species whose molar extinction coefficient in this region is smaller than that of octopus rhodopsin. The lifetime (τ) of the transient species in H_2O suspension was estimated from the following equation:

$$\tau/\Delta t \sim \Delta A/\Delta\epsilon\, c^*\ell.$$

Here Δt and ΔA denote the resolution time of the apparatus (36 ps) and the measured absorbance change at 430 nm (−0.008, *solid curve* in Fig. 3 *b*), respectively. The difference between the molar extinction coefficient of the transient (ϵ^*) and that of rhodopsin in the ground state (ϵ^R) is denoted by $\Delta\epsilon$ ($=\epsilon^* - \epsilon^R$). The upper limit for $|\Delta\epsilon|$ is equal to ϵ^R at 430 nm (19,200 M^{-1} cm^{-1}). Optical path length is denoted by ℓ (0.2 cm). The concentration of the transient c^* was taken to be (6.8 ± 0.7) × 10^{-5} M on the assumption that the formation yield of the transient is unity. Thus the lifetime was estimated to be longer than 1 ps. This value is much longer than the reported fluorescence lifetime of bovine rhodopsin, which is on the order of 0.1 ps (23). Therefore, we attribute the initial change to the formation of a short-lived ground state intermediate. We tentatively call the intermediate "primerhodopsin."

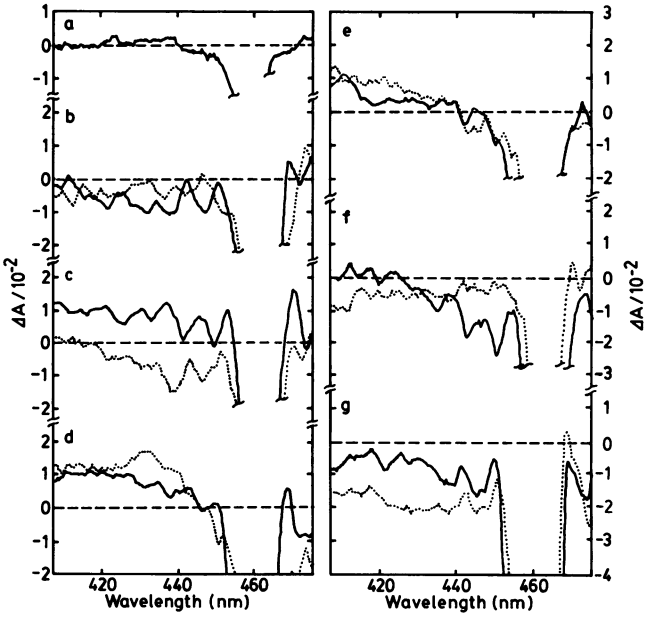

FIGURE 3 Picosecond difference absorption spectra of octopus rhodopsin in H_2O (*solid curve*) and in D_2O (*dotted curve*) suspensions after 461-nm excitation at 8°C. (*a*) Base line, (*b*) 0 ps, (*c*) 15 ps, (*d*) 30 ps, (*e*) 100 ps, (*f*) 150 ps, (*g*) 500 ps. 30–40 pairs of excitation and nonexcitation data were averaged. The excitation photon density is (9.3 ± 1.3) × 10^{15} photons/cm^2.

The spectra 30 ps after excitation (Fig. 3 *d*) clearly indicate the formation of hypsorhodopsin in both the H_2O and D_2O suspensions. Bleaching was observed 500 ps after excitation (Fig. 3 *g*). The spectral changes between 30 and 500 ps are caused by the decay of hypsorhodopsin to the next intermediate bathorhodopsin.

The formation of bathorhodopsin is clearly shown by the difference absorption spectrum 1 ns after the excitation of octopus rhodopsin in the H_2O suspension at 8°C (Fig. 4, *dotted curve*). The wavelength of the maximum absorbance change in the difference spectrum is 550 nm. This is in reasonable agreement with the wavelength of the

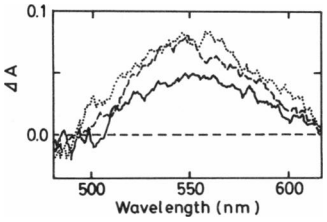

FIGURE 4 Picosecond difference absorption spectra of octopus rhodopsin in H_2O suspension after 461-nm excitation at 8°C. *Solid curve*, −22 ps; *dashed curve*, 100 ps; *dotted curve*, 1 ns. 20–30 pairs of excitation and nonexcitation data were averaged. The excitation density is (1.9 ± 0.3) × 10^{16} photons/cm^2.

bathorhodopsin-minus-rhodopsin difference spectrum at 10 K obtained from Fig. 1.

The time-dependencies of the absorbance change at 430 nm both in the H_2O (*open circles*) and in D_2O (*solid circles*) suspensions are shown in Fig. 5 *a*. The formation rate of hypsorhodopsin in the D_2O suspension is slower than in H_2O. Hypsorhodopsin decays to bathorhodopsin with a time constant of several 10 ps in both the H_2O and D_2O suspensions. The formation time of bathorhodopsin was measured to be ~70 ps ($[1.4 \pm 0.6] \times 10^{10}$) by monitoring the absorbance change at 560 nm. These results are consistent with those reported (7, 8, 16–18).

The solid curve in Fig. 4 exhibits a transient spectrum 22 ps before excitation. The observed absorbance change is due to the overlap of the tailing part of the probe pulse (30-ps fwhm) and the leading edge of the excitation pulse (20-ps fwhm). The concentration of the initially formed species is higher than that of bathorhodopsin. The spectrum at −22 ps is not attributed to octopus rhodopsin in the excited state but an intermediate in the ground state "primerhodopsin," which corresponds to Batho' (6, 9), a deeply red-shifted precursor (7, 8), and photorhodopsin (10) because its lifetime is longer than the fluorescence lifetime of rhodopsin (23). Fig. 5 *b* shows the temporal shift of the wavelength λ_g $[= \int_{500}^{600} \lambda \Delta A(\lambda) d\lambda / \int_{500}^{600} \Delta A(\lambda) d\lambda]$. The rapid blue-shift of the spectrum corresponds to the build-up of the absorbance at 430 nm. It suggests hypsochromic shift taking place, i.e., primerhodopsin to hypsorhodopsin conversion. Kobayashi (7, 8) found that the difference spectrum of bovine primerhodopsin minus rhodopsin is red-shifted from the difference spectrum of bovine bathorhodopsin minus rhodopsin by ~20 nm. Such a large spectral shift from octopus bathorhodopsin to primerhodopsin was not found in the present study.

Fig. 6 shows the dependence of the absorbance change at 430 ± 10 nm on the excitation photon density. Solid lines are obtained by numerical calculations described in the later section.

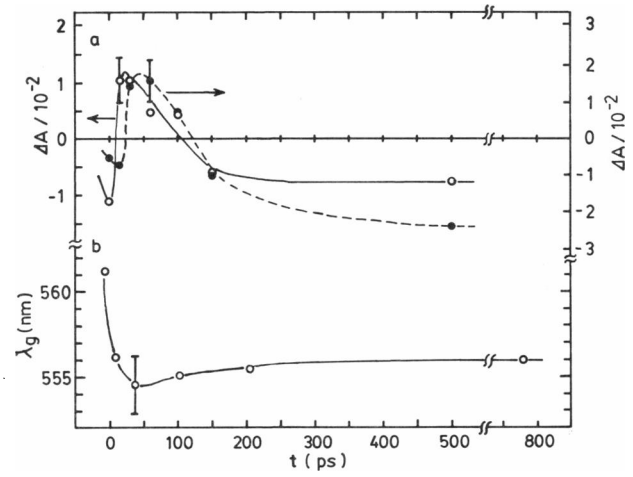

FIGURE 5 (*a*) Time-dependence of the transient absorption change of octopus rhodopsin in H_2O and in D_2O suspensions after 461-nm excitation at 8°C. The averaged absorbance change between 420 and 440 nm are plotted for H_2O (*open circles*) and D_2O (*closed circles*) suspensions. The excitation photon density is $(9.3 \pm 1.3) \times 10^{15}$ photons/cm^2. (*b*) Time-dependence of the wavelength λ_g of difference absorption spectrum following 461-nm excitation at 8°C. The λ_g is calculated by the following equation. $\lambda_g = \int_{500}^{600} \lambda \Delta A(\lambda) d\lambda / \int_{500}^{600} \Delta A(\lambda) d\lambda$. The excitation photon density is $(1.9 \pm 0.3) \times 10^{16}$ photons/cm^2.

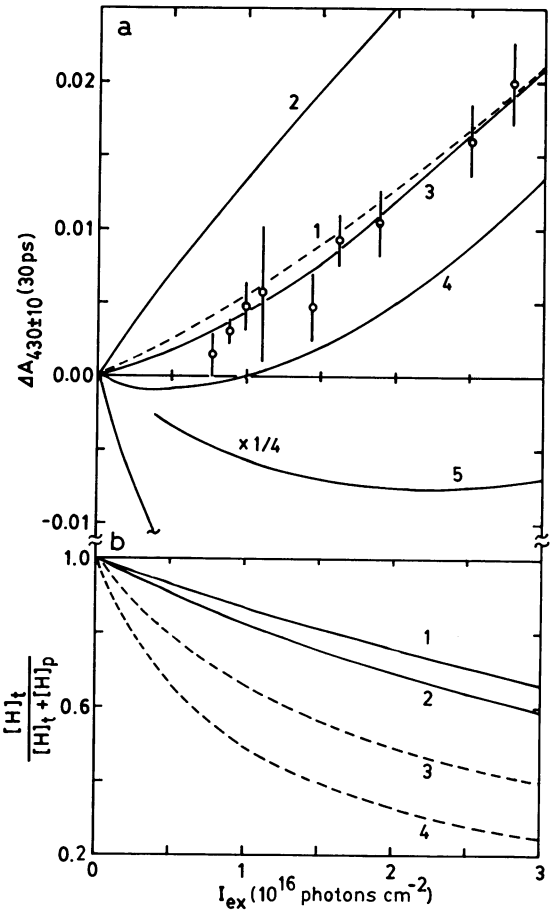

FIGURE 6 (*a*) Excitation energy dependence of the transient absorption 30 ps after excitation monitored at 430 ± 10 nm. The efficiency for the hypsorhodopsin formation by the thermal decay of primerhodopsin, ϕ_H $[= k_H/(k_H + k_B)]$, is varied from 1 (curves *1* and *2*), 0.8 (curve *3*), 0.7 (curve *4*), to 0 (curve *5*). Lifetimes of primerhodopsin and hypsorhodopsin are set at 15 and 70 ps, respectively. The quantum yield for the formation of primerhodopsin, η_P, is set at 0.5. The absorption cross-sections σ^R and σ^P at 461 nm are 1.08×10^{-16} and 0.48×10^{-16} cm^2, respectively, for curve *1*. The absorption cross-sections of rhodopsin (σ^R) and primerhodopsin (σ^P) at 461 nm are set at 1.08×10^{-16} and 0.96×10^{-16} cm^2, respectively, for curves *2–5*. (*b*) The molar fraction of hypsorhodopsin thermally formed out of the total hypsorhodopsin formed. Parameters η_P, τ_P, and τ_H are taken as the same values used for the calculation of curves *2–5* in Fig. 6 *a*. The efficiency ϕ_H are set at 1 (curve *1*) and 0.7 (curve *2*) for 461-nm excitation and 1 (curve *3*) and 0.5 (curve *4*) for 532-nm excitation. The absorption cross-sections of rhodopsin (σ^R) and primerhodopsin (σ^P) at 532 nm are set at 0.38×10^{-16} and 1.25×10^{-16} cm^2, for curves *3* and *4*, respectively.

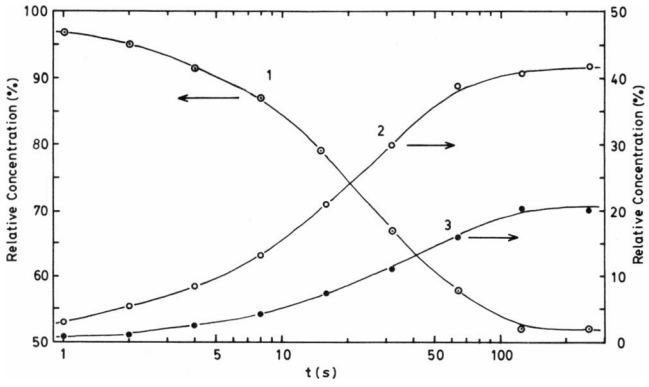

FIGURE 7 Photolysis of octopus rhodopsin by 480-nm continuous irradiation at 10 K. Curve *1*, octopus rhodopsin; curve *2*, bathorhodopsin; curve *3*, hypsorhodopsin.

Low Temperature Irradiation of Octopus Rhodopsin

To estimate the concentrations of the hypsorhodopsin and bathorhodopsin formed during the early stages of illumination at 10 K, octopus rhodopsin was irradiated for a short time with 480-nm light. Hypsorhodopsin was detected well above the detection limit by the illumination of 480-nm light for 1 s (Fig. 7). The formation yield of hypsorhodopsin is much smaller than that of bathorhodopsin at 10 K as shown in Fig. 7. The ratio of the molar fractions of hypsorhodopsin and bathorhodopsin formed by 1-s light exposure was ⅓. In the previous work, Tsuda et al. (15) reported that bathorhodopsin appears before the significant spectral change due to hypsorhodopsin formation is found (2,048 s of irradiation). The formation yield of hypsorhodopsin by steady-state irradiation was smaller than that of bathorhodopsin. The concentrations of hypsorhodopsin and bathorhodopsin were 9×10^{-6} and 1.3×10^{-5} M, respectively, when octopus rhodopsin was irradiated by 530-nm light for 8 s (Fig. 1 in reference 15).

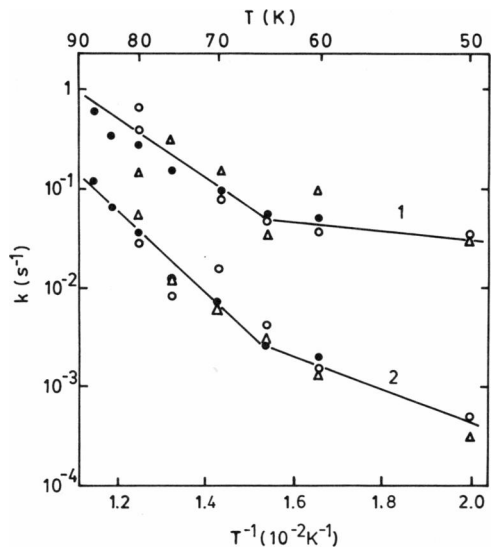

FIGURE 8 Arrhenius plot of the decay of hypsorhodopsin monitored at 440 nm. *Open circles*, sonicated membrane suspension in H_2O; *closed circles*, sonicated membrane suspension in D_2O; *triangles*, rhodopsin extracted by a detergent (2% L-1690).

Octopus hypsorhodopsin is converted to bathorhodopsin when the temperature is increased above 45 K (15). The decay kinetics of hypsorhodopsin monitored at 440 nm can be fitted fairly well by the sum of two exponential decay functions at given temperatures (15). Fig. 8 shows the Arrhenius plot of the decay of hypsorhodopsin in the H_2O (*open circles*) and D_2O (*solid circles*) suspensions and a sample extracted with the detergent L-1690 (*triangles*). Temperature dependence of the decay rate of fast and slow components in 50–65 K region agrees with that (53–73 K) reported previously (15). The decay rates of both components depend on temperature more sensitively in the 65–80 K region than in the 50–65 K region. The kinetic behavior of the extracted sample (*triangles*) is the same as that of the sonicated membrane (*open circles*). There was no H_2O/D_2O exchange effect on the rate of the conversion from hypsorhodopsin to bathorhodopsin.

Numerical Calculations

Numerical calculations were performed to interpret the observed excitation photon density dependence of the absorbance change induced by a 20-ps (fwhm) excitation light pulse. A model for the calculations is shown in Fig. 9. This model is based on the following schemes. (*a*) Primerhodopsin (Batho' or photorhodopsin) is the first intermediate in the primary process of the photobleaching reaction of rhodopsin. (*b*) Bathorhodopsin and hypsorhodopsin can be thermally formed from primerhodopsin with rate constants of k_B and k_H, respectively. (*c*) Hypsorhodopsin can be photochemically formed from primerhodopsin.

The rate constants k^*_{Ph}, k_R, k_P, and k'_H are much larger than the inverse of the excitation pulse width. The temporal pulse shapes of the probe and excitation pulses were assumed to be Gaussian functions with 20 and 30 ps fwhm,

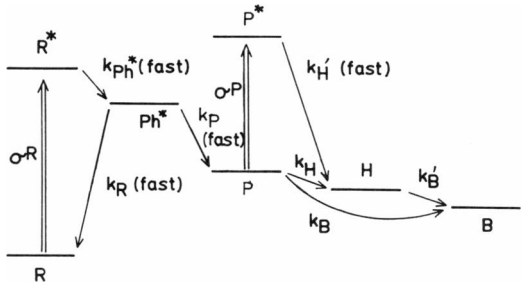

FIGURE 9 Kinetic scheme of the primary process of rhodopsin for numerical calculations. Rhodopsin, primerhodopsin, bathorhodopsin, and hypsorhodopsin are denoted by R, P, B, and H, respectively. Rhodopsin in the excited singlet state with 90° twisted C_{11}-C_{12} bond (phantom state) is denoted by Ph*. The rate constant and the absorption cross-section at excitation wavelength are denoted by k and σ, respectively.

respectively. The spatial intensity distributions of the probe and excitation pulses were also assumed to be Gaussian functions with 0.4 and 1.2 mm fwhm, respectively. Details of the calculation are shown in the Appendix.

Curves *1–5* in Fig. 6 *a* show the calculated excitation density dependence for several values of ϕ_H [$=k_H/(k_H + k_B)$], the efficiency for the thermal formation of hypsorhodopsin. The lifetime of primerhodopsin, τ_P [$=1/(k_H + k_B)$], was set at that of the lifetime of bovine primerhodopsin, 15 ps (7, 8). The quantum yield for the formation of primerhodopsin, η_P, was taken to be the same as that for the bleaching of octopus rhodopsin 0.5 (Tsuda, M., B. Mao, and T. G. Ebrey, unpublished results). The lifetime of hypsorhodopsin, τ_H ($=1/k'_B$), was taken to be 70 ps from the formation time of bathorhodopsin monitored at 560 nm. The absorption cross-section of primerhodopsin (σ^P) in the 410–480 nm region is smaller than that of octopus rhodopsin (Fig. 3 *b*). When the σ^P values at both excitation and probe wavelength (461 and 430 nm, respectively) were set to those of bathorhodopsin, the values of the calculated absorbance change for $\phi_H = 1$ (Fig. 6 *a*, curve *1*) fit the experimental results. The absorption cross-section of primerhodopsin at excitation wavelength (461 nm) was set to be twice that of bathorhodopsin ($\sigma^P = 2\,\sigma^B = 0.87\,\sigma^R$) for curves *2–5*. Curve *5* in the figure was calculated for $\phi_H = 0$. This parametrization corresponds to the case when hypsorhodopsin is formed only by a photochemical reaction of primerhodopsin and that bathorhodopsin is directly formed from primerhodopsin. An intense bleaching at 430 nm is predicted for an excitation photon density lower than 3×10^{16} photons/cm^2. This is not found experimentally and so the thermal conversion from primerhodopsin to hypsorhodopsin must also be considered. Curves *2*, *3*, and *4* were calculated for $\phi_H = 1$, 0.8, and 0.7, respectively. Curve *2* agrees well with the experimental results.

The molar fraction of the hypsorhodopsin thermally formed from primerhodopsin, $f_t = [H]_t/([H]_t + [H]_p)$, was calculated (Fig. 6 *b*). Here, parameters η_P, τ_P, σ^P, and τ_H were taken as the same as values used for the calculation of curves *2–5* in Fig. 6 *a*. The fraction of the thermally formed hypsorhodopsin obtained by the 532-nm excitation of octopus rhodopsin (curves *3* and *4*) is smaller than that by the 461-nm excitation (curves *1* and *2*) when the excitation photon densities are equal.

Further calculations were performed using the range of values for η_P, τ_P, σ^P, and τ_H shown in Table I. The calculated excitation photon density dependence of the absorbance change 30 ps after excitation sensitively depend on τ_P [$=1/(k_H + k_B)$] and σ^P at the excitation wavelength and weakly depend on η_P and τ_H. The lowest ϕ_H value was obtained when τ_P was set at 15 ps. When τ_P was assumed to be as long as 200 ps (18), the calculated absorbance change 30 ps after excitation monitored at 430 nm was much smaller than the observed value even if ϕ_H was set at the upper limit 1.0. The lower limit of the fitted ϕ_H was obtained when the σ^P values at 430 and 461 nm were assumed to be equal to those of octopus rhodopsin. All the ϕ_H values that fit the experimental data were larger than 0.6. Therefore we conclude that a majority of the hypsorhodopsin is formed thermally from primerhodopsin, and that hypsorhodopsin is formed even under low excitation photon density at room temperature.

TABLE I
PARAMETERS USED IN THE NUMERICAL CALCULATIONS

η_P*	τ_P/ps‡	γ_λ§	τ_H/ps‖
0.5, 0.6, 0.7	10, 15, 30, 200	1, 2	50, 60, 70, 100

*Formation yield of primerhodopsin, $\eta_P = k_P/(k_P + k_R)$. The lower value 0.5 was estimated by Tsuda and Ebrey (unpublished results). The upper limit 0.7 was taken from the quantum yield for the formation of bovine bathorhodopsin (0.67 [25, 26]).
‡Lifetime of primerhodopsin, $\tau_P = 1/(k_H + k_B)$.
§Absorption cross-section of primerhodopsin at the excitation wavelength (σ^P) is given by $\sigma^P = \gamma\sigma^B$. Here σ^B is cross-section of bathorhodopsin. The upper limit of γ is 2.3 because σ^P is smaller than the absorption cross-section of octopus rhodopsin in 420–480-nm region.
‖Lifetime of hypsorhodopsin, $\tau_H = 1/k'_B$.

DISCUSSION

Formation of Primerhodopsin

The primary photoprocess of rhodopsin is initiated by the rapid photoisomerization of retinal. The absorption spectrum of rhodopsin in the excited singlet state has not been measured because of its short lifetime. The fluorescence lifetime of bovine rhodopsin is on the order of 0.1 ps (23). Kobayashi found a deeply red-shifted precursor in the photolysis of bovine rhodopsin with 530-nm excitation light (6-ps fwhm) at room temperature, and attributed it to rhodopsin in the lowest excited singlet state. However, the lifetime (15 ± 5 ps) is longer than the upper limit of the fluorescence lifetime estimated from the fluorescence quantum yield (1×10^{-5}) (23). The precursor is a ground state species primerhodopsin which is the same as Batho' (9) found by Peters et al. (6) at low temperature. In the present study, we observed the formation of primerhodopsin at 8°C. The lifetime of primerhodopsin was estimated to be smaller than the resolution time of our apparatus (36 ps) and longer than 1 ps, which is consistent with the reported lifetime of bovine primerhodopsin (15 ± 5 ps [7, 8]) and is shorter than the lifetime of squid primerhodopsin (~ 200 ps [18]).

Formations of Hypsorhodopsin and Bathorhodopsin

As already mentioned in the previous section, it has been proposed that hypsorhodopsin is only formed photochemically from primerhodopsin (18). However, it had not been clarified whether or not hypsorhodopsin can be formed

thermally with excitation photon density low enough for the excitation of primerhodopsin to be avoided. The present study showed that both hypsorhodopsin and bathorhodopsin are thermally formed from primerhodopsin. A considerable amount of hypsorhodopsin was formed in the photolysis of octopus rhodopsin with a low excitation photon density at 461 nm (7.7×10^{15} photons/cm^2, 0.3 photons/molecule). The molar fractions of hypsorhodopsin formed thermally (ft) and photochemically (f_p) from primerhodopsin are estimated to be 0.9 and 0.1, respectively (see Fig. 6 *b*). If the excitation wavelength is 532 nm, the excitation photon density must be lower than 4.5×10^{15} photons/cm^{-2} to avoid an appreciable amount of hypsorhodopsin photochemically formed from the primerhodopsin ($f_p < 0.1$).

The efficiency for the photochemical conversion from primerhodopsin to hypsorhodopsin is increased with the excitation intensity as reported by Matuoka et al. (18). The following other possibilities for the multiphoton mechanisms for the formation of hypsorhodopsin were considered: (*a*) simultaneous two-photon excitation of rhodopsin, and (*b*) the absorption of a second photon by rhodopsin in the excited singlet state. Birge et al. reported that rhodopsin has a large cross-section for the two-photon absorption (19). However the ratio of the efficiency for the two-photon absorption to that for one-photon absorption may be small because of the intense one-photon absorption of rhodopsin at the excitation wavelength 461 nm. The numerical calculations result that the efficiency for the formation of hypsorhodopsin by two-step excitation process sensitively depends on the lifetime of the species that absorbs a second photon. The absorption of a second photon by rhodopsin in the excited state in negligible small because of its short lifetime.

The thermal formation of hypsorhodopsin was also found using 480-nm continuous irradiation of octopus rhodopsin at 10 K. Hypsorhodopsin is formed in the initial stage of irradiation before the accumulation of any species that could be photochemically converted to hypsorhodopsin. The photochemical formation of hypsorhodopsin from the primerhodopsin could not occur because of the low excitation power and the short lifetime of primerhodopsin (29 ± 2 ps for bovine Batho' at 10 K [6]). The above results at physiological and low temperatures show that hypsorhodopsin is thermally formed from primerhodopsin. The primary photoprocess of octopus rhodopsin is given as the following "thermal" reactions initiated by the photoisomerization of retinal.

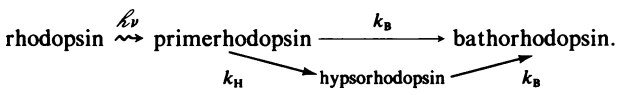

The conversion efficiencies from primerhodopsin to bathorhodopsin and hypsorhodopsin ($\phi_B = k_B/[k_B + k_H]$ and $\phi_H = 1 - \phi_B$, respectively) in octopus rhodopsin were found to be smaller than 0.4 and larger than 0.6, respectively, at 8°C. These values are consistent with the values of ϕ_H (>0.75) and ϕ_B (<0.25) in bovine rhodopsin at room temperature (7, 8). On the other hand the ϕ_H value is ~0.25 at 10 K. Therefore it is concluded that the rate of the primerhodopsin → hypsorhodopsin conversion (k_H) depends more sensitively on temperature than that of the primerhodopsin → bathorhodopsin conversion (k_B).

Peters et al. (6) reported that the lifetime of bovine primerhodopsin (Batho') is about seven times longer in a D_2O suspension than in H_2O. In the present study, we found that the formation of hypsorhodopsin is slower in D_2O than in H_2O. These two results show that the decay rate constant of primerhodopsin, k_p ($= \tau_P^{-1} = k_H + k_B$), is affected by H_2O/D_2O exchange. We could not obtain any definitive isotope effect on the formation yield of hypsorhodopsin at 8°C within experimental error. On the other hand Pande et al. (24) found that the molar fraction of hypsorhodopsin in the photo-steady state at 12 K is 1.4–1.8 times larger in a D_2O suspension than in H_2O using resonance Raman studies. The increases in the lifetime of primerhodopsin and formation yield of hypsorhodopsin in a D_2O suspension indicate that the H_2O/D_2O exchange decreases the rate of the decay of primerhodopsin to bathorhodopsin (k_B) more efficiently than the decay to hypsorhodopsin (k_H). There is no information whether or not proton transfer occurs in the primerhodopsin → hypsorhodopsin conversion as speculated by Honig et al. (9). There may be a H_2O/D_2O effect on the interaction between the chromophore and surroundings which affects the decay dynamics of primerhodopsin. The decay to bathorhodopsin is the main decay process of primerhodopsin ($k_B > k_H$) at 10 K. Therefore the decrease in k_B in D_2O causes the increase in the amount of hypsorhodopsin formed, ϕ_H. On the other hand, k_B is smaller than k_H at 8°C. The H_2O/D_2O exchange effect in ϕ_H is smaller at 8°C than at 10 K.

No isotope effect was found in the rate of the hypsorhodopsin → bathorhodopsin conversion (see Fig. 8). The rate-determining steps for the primerhodopsin → hypsorhodopsin and hypsorhodopsin → bathorhodopsin conversions may be a conformational change in opsin which affects the interaction between an amino acid residue and retinal.

APPENDIX

Numerical calculations were performed with the following equations on the basis of the model in Fig. 9.

$$d[R]/dt = -I_e(t)\,\sigma^R\,\eta_P\,[R] \quad \text{(A1)}$$

$$d[P]/dt = I_e(t)\,\sigma^R\,\eta_P\,[R] - [k_B + k_H + I_e(t)\,\sigma^P\,\eta_H]\,[P] \quad \text{(A2)}$$

$$d[H]/dt = k_H\,[P] - k'_B\,[H] + I_e\,\sigma^P\,\eta_H\,[P] \quad \text{(A3)}$$

$$d[B]/dt = k_B\,[P] + k'_B\,[H] \quad \text{(A4)}$$

$$I_e(t) = (E/\sqrt{\pi}\,G_e)\exp(-t^2/G_e^2). \quad \text{(A5)}$$

Here R, Ph*, P, H, and B denote rhodopsin in the ground state and the phantom excited singlet state, primerhodopsin, hypsorhodopsin, and bathorhodopsin, respectively. The temporal pulse shape of excitation light was assumed to be Gaussian function with 20-ps fwhm. The photon number of the excitation pulse is denoted by E. The absorption cross-sections of rhodopsin and primerhodopsin at the excitation wavelength are denoted by σ^R and σ^P, respectively. The quantum yield for the formation of primerhodopsin is denoted by η_P. The quantum yield η_H for the formation of hypsorhodopsin from primerhodopsin photochemically is taken to be 1.0, the maximum possible. The rate constants k^*_{Ph}, k_R, k_P, and k'_H do not appear in the differential equations because they are much larger than the inverse of the excitation pulse width (20-ps fwhm). The absorbance change at wavelength λ and delay time t is calculated with the following equations:

$$\Delta A_\lambda(t) = \log\left[\int_{-\infty}^{\infty} I_p(t, t')\,dt' \Big/ \int_{-\infty}^{\infty} I_p(t, t')10^{-A_\lambda(t')}\,dt'\right] - \epsilon^R_\lambda [R]_{t=-\infty}\ell \quad \text{(A7)}$$

$$A_\lambda(t') = \{\epsilon^R_\lambda [R] + \epsilon^P_\lambda [P] + \epsilon^H_\lambda [H] + \epsilon^B_\lambda [B]\}\ell \quad \text{(A8)}$$

$$I_p(t, t') = (1/\sqrt{\pi}\, G_p) \exp\,[-(t' - t)^2/G_p^2]. \quad \text{(A9)}$$

Here $[R]_{t=-\infty}$ and $I_p(t', t)$ show the concentration of rhodopsin before excitation and the temporal pulse shape of probe light with 30-ps fwhm. Molar extinction coefficient and optical path length are denoted by ϵ and ℓ, respectively.

The authors thank Mr. Koshihara for his help in the early stage of picosecond experiment and Drs. Uchiki and Yoshizawa for their help in constructing the data-analyzing system of micro- and mini-computers.

This work was partly supported by a Grant in Aid for Special Distinguished Research (56222005) and a Special Research Project (60115004) to T. Kobayashi and a Grant-in-Aid (60115001) to M. Tsuda from the Ministry of Education, Science, and Culture in Japan. It was also supported partly by the Toray Science and Technology Foundation and Kurata Science Foundation to T. Kobayashi and the JSPS-NSF Japan-US Cooperative Science Program to M. Tsuda and T. G. Ebrey.

Received for publication 15 June 1987 and in final form 2 September 1987.

REFERENCES

1. Ohtani, H., T. Kobayashi, M. Tsuda, and S. Koshihara. 1984. Picosecond spectroscopy of octopus rhodopsin. *Proc. Intl. Conference Fast Reactions Biol. Systems.* Kyoto, Japan. 98–99.
2. Hubbard, R., and A. Kropf. 1958. The action of light on rhodopsin. *Proc. Natl. Acad. Sci. USA.* 44:130–139.
3. Yoshizawa, T., and G. Wald. 1963. Pre-lumirhodopsin and the bleaching of visual pigments. *Nature (Lond.).* 197:1279–1286.
4. Yoshizawa, T. 1972. The behavior of visual pigments at low temperatures. *In* Handbook of Sensory Physiology VII/1. H. J. A. Dartnall, editor. Springer-Verlag, Berlin. 146–179.
5. Yoshizawa, T., and Y. Kitô. 1958. Chemistry of the rhodopsin cycle. *Nature (Lond.).* 182:1604–1605.
6. Peters, K., M. L. Applebury, and P. M. Rentzepis. 1977. Primary photochemical event in vision: proton translocation. *Proc. Natl. Acad. Sci. USA.* 74:3119–3123.
7. Kobayashi, T. 1980. Hypsorhodopsin: the first intermediate of the photochemical process in vision. *FEBS (Fed. Eur. Biochem. Soc.) Lett.* 106:313–316.
8. Kobayashi, T. 1980. Existence of hypsorhodopsin as the first intermediate in the primary photochemical process of cattle rhodopsin. *Photochem. Photobiol.* 32:207–215.
9. Honig, B., T. Ebrey, R. H. Callender, U. Dinur, and M. Ottolenghi. 1979. Photoisomerization, energy storage, and charge separation: a model for light energy transduction in visual pigments and bacteriorhodopsin. *Proc. Natl. Acad. Sci. USA.* 76:2503–2507.
10. Shichida, Y., S. Matuoka, and T. Yoshizawa. 1984. Formation of photorhodopsin, a precursor of bathorhodopsin, detected by picosecond laser photolysis at room temperature. *Photobiochem. Photobiophys.* 7:221–228.
11. Busch, G. E., M. L. Applebury, A. A. Lamola, and P. M. Rentzepis. 1972. Formation and decay of prelumirhodopsin at room temperatures. *Proc. Natl. Acad. Sci. USA.* 69:2802–2806.
12. Sundstrom, V., P. M. Rentzepis, K. Peters, and M. L. Applebury. 1977. Kinetics of rhodopsin at room temperature measured by picosecond spectroscopy. *Nature (Lond.).* 267:645–646.
13. Green, B. H., T. G. Monger, R. R. Alfano, B. Aton, and R. H. Callender. 1977. Cis-trans isomerization in rhodopsin occurs in picoseconds. *Nature (Lond.).* 269:179–180.
14. Shichida, Y., F. Tokunaga, and T. Yoshizawa. 1979. Squid hypsorhodopsin. *Photochem. Photobiol.* 29:343–351.
15. Tsuda, M., F. Tokunaga, T. G. Ebrey, K. T. Yue, J. Marque, and L. Eisenstein. 1980. Behavior of octopus rhodopsin and its photoproducts at very low temperatures. *Nature (Lond.).* 287:461–462.
16. Shichida, Y., T. Yoshizawa, T. Kobayashi, H. Ohtani, and S. Nagakura. 1977. Squid hypsorhodopsin and bathorhodopsin by a picosecond laser photolysis. *FEBS (Fed. Eur. Biochem. Soc.) Lett.* 80:214–216.
17. Shichida, Y., T. Kobayashi, T. Yoshizawa, H. Ohtani, and S. Nagakura. 1978. Picosecond laser photolysis of squid rhodopsin at room and low temperatures. *Photochem. Photobiol.* 24:335–341.
18. Matuoka, S., Y. Shichida, and T. Yoshizawa. 1984. Formation of hypsorhodopsin at room temperature by picosecond green pulse. *Biochim. Biophys. Acta.* 765:38–42.
19. Birge, R. R., L. P. Murray, B. M. Pierce, H. Akita, V. Balogh-Nair, L. A. Finden, and K. Nakanishi. 1985. Two-photon spectroscopy of locked-11-*cis*-rhodopsin: evidence for a protonated Schiff base in a neutral protein binding site. *Proc. Natl. Acad. Sci. USA.* 82:4117–4121.
20. Iwai, J., M. Ikeuchi, Y. Inoue, and T. Kobayashi. 1984. Early processes of protochlorophyllide photoreduction as measured by nanosecond and picosecond spectrophotometry. *In* Protochlorophyllide Reduction and Greening. C. Sironval and M. Brouers, editors. Martinus Nijhoff/Dr. W. Junk Publishers, Hague. 99–112.
21. Tsuda, M. 1979. Transient spectra of intermediates in the photolytic sequence of octopus rhodopsin. *Biochim. Biophys. Acta.* 545:537–546.
22. Nashima, K., M. Mitsudo, and Y. Kitô. 1978. Fatty acid esters of sucrose as effective detergents. *Biochim. Biophys. Acta.* 536:78–87.
23. Doukas, A. G., M. R. Junnarkar, R. R. Alfano, R. H. Callender, T. Kakitani, and B. Honig. 1984. Fluorescence quantum yield of visual pigments: evidence for subpicosecond isomerization rates. *Proc. Natl. Acad. Sci. USA.* 81:4790–4794.
24. Pande, A. J., R. H. Callender, T. G. Ebrey, and M. Tsuda. 1984. Resonance Raman study of the primary photochemistry of visual pigments. Hypsorhodopsin. *Biophys. J.* 45:573–576.
25. Dartnall, H. J. A. 1972. Handbook of Sensory Physiology VII/1. H. J. A. Dartnall, editor. Springer-Verlag, Berlin. 122–145.
26. Hurley, J., T. G. Ebrey, B. Honig, and M. Ottolenghi. 1977. Temperature and wavelength effects on the photochemistry of rhodopsin, isorhodopsin, bacteriorhodopsin, and their photoproducts. *Nature (Lond.).* 270:540–542.